New developments in the imaging of lung cancer

Ádám Domonkos Tárnoki[1,2], Dávid László Tárnoki[1,2], Marta Dąbrowska[3], Magdalena Knetki-Wróblewska[4], Armin Frille[5], Harrison Stubbs[6,7], Kevin G. Blyth[6,7] and Amanda Dandanell Juul[8]

[1]Medical Imaging Centre, Semmelweis University, Budapest, Hungary. [2]National Tumour Biology Laboratory, Oncologic Imaging and Invasive Diagnostic Centre, National Institute of Oncology, Budapest, Hungary. [3]Department of Internal Medicine, Pulmonary Diseases and Allergy, Medical University of Warsaw, Warsaw, Poland. [4]Maria-Sklodowska Curie National Research Institute of Oncology, Warsaw, Poland. [5]Department of Respiratory Medicine, University Hospital Leipzig, Leipzig, Germany. [6]Glasgow Pleural Disease Unit, Queen Elizabeth University Hospital, Glasgow, UK. [7]School of Cancer Sciences, University of Glasgow, Glasgow, UK. [8]Departments of Respiratory Medicine, Odense University Hospital, Odense, Denmark.

Corresponding author: Ádám Domonkos Tárnoki (tarnoki2@gmail.com)

Shareable abstract (@ERSpublications)
Radiological and nuclear medicine methods play a fundamental role in the diagnosis and staging of patients with lung cancer. Imaging is essential in the detection, characterisation, staging and follow-up of lung cancer. https://bit.ly/3Ul78K9

Cite this article as: Tárnoki ÁD, Tárnoki DL, Dąbrowska M, *et al*. New developments in the imaging of lung cancer. *Breathe* 2024; 20: 230176 [DOI: 10.1183/20734735.0176-2023].

Received: 12 Oct 2023
Accepted: 25 Jan 2024

Abstract

Radiological and nuclear medicine methods play a fundamental role in the diagnosis and staging of patients with lung cancer. Imaging is essential in the detection, characterisation, staging and follow-up of lung cancer. Due to the increasing evidence, low-dose chest computed tomography (CT) screening for the early detection of lung cancer is being introduced to the clinical routine in several countries. Radiomics and radiogenomics are emerging fields reliant on artificial intelligence to improve diagnosis and personalised risk stratification. Ultrasound- and CT-guided interventions are minimally invasive methods for the diagnosis and treatment of pulmonary malignancies. In this review, we put more emphasis on the new developments in the imaging of lung cancer.

Educational aims

- To understand the current knowledge on imaging methods in the detection, characterisation, staging and follow-up of patients with lung cancer.
- To learn about the role of low-dose chest CT screening.
- To understand the rationale of biomarkers, radiomics, radiogenomics and artificial intelligence in the diagnostic and treatment pathways for lung cancer.
- To learn the role of ultrasound- and CT-guided interventions in the diagnosis and treatment of lung cancer.

Epidemiology of lung cancer

According to GLOBOCAN 2020 (global cancer statistics), it is estimated that 2.2 million new cases of lung cancer were diagnosed worldwide in the year 2020. It is the most common cancer in men (14.3% of all cancers), and the third most common cancer in women (after breast cancer and colorectal cancer) with an incidence of about 8.4% of all cancers [1]. Moreover, lung cancer is the leading cause of cancer death worldwide, with 1.8 million deaths in 2020, which was estimated as 18% of all cancer deaths (the most common cancer death in men (21%) and the second in women (13.7%)) [1]. The age-standardised incidence rates per 100 000 vary by sex and by region of the world, ranging from 2.8 in West Africa to 41.7 in Western Europe and 51.6 in Micronesia/Polynesia for men, and from 1.8 in West Africa to 25 in Western Europe and 30.1 in North America for women [1].

Introduction to the imaging methods in lung cancer diagnostics

Imaging plays a fundamental role in the diagnosis and staging of patients with lung cancer. In everyday practice, combination of several imaging studies, namely conventional chest radiography, chest computed tomography (CT), magnetic resonance imaging (MRI) and nuclear medicine techniques, mainly positron emission tomography (PET), is needed to ensure the detection, characterisation, staging and follow-up of lung cancer [2]. In addition, there is increasing evidence for the role of low-dose CT (LDCT) screening of the chest in the early detection of pulmonary malignancies, beyond the routine chest radiographs. In addition, radiomics and radiogenomics are emerging fields, reliant on artificial intelligence (AI), which offer great potential to improve diagnosis and personalised risk stratification, thus having a major impact on diagnostic and treatment pathways for lung cancer [3]. Ultrasound- and CT-guided interventions are minimally invasive and established methods for the diagnosis of pulmonary lesions. In this review, the use of these imaging techniques in lung cancer management will be discussed.

The role of chest radiography in diagnosis and follow-up

Chest radiography is the first and most commonly performed imaging method during the workup of suspected lung cancer in symptomatic patients, and it plays a role in the follow-up as well. Its advantages include its widespread availability, technical feasibility, simplicity, low radiation, low risk and low cost [4]. Routine chest radiography includes bilateral views and postero-anterior and lateral projections, with the patient in a standing position. Chest radiography is performed with the hard beam technique (120–130 kV, 5 mAs) from a focus-film distance of 2 m, with deep inhalation. Fluoroscopy is an additional imaging examination if the diagnosis is questionable on the chest radiograph. The radiation exposure of the fluoroscopy is high, its spatial resolution is poor, and its assessment is subjective and it may be insufficiently documented. An antero-posterior or a Frimann-Dahl scan taken in the side-lying position may be necessary for a patient in poor condition.

As soon as chest radiography has been performed, post-processing techniques can be used to improve image quality on digital images, giving the potential for dose reduction [5, 6]. Magnification, windowing and greyscale inversion might be helpful techniques for better identification. Other post-processing techniques include temporal subtraction and dual-energy subtraction, in order to increase the accuracy of detection of lung nodules, especially on lung cancer screening [4, 7]. A comparison of conventional and digital chest radiography is shown in table 1.

Chest radiography has not been shown to decrease mortality when used for lung cancer screening, and it is less effective compared to LDCT, although chest radiography is one of the most commonly utilised diagnostic tools for chest diseases in clinical practice [2]. The sensitivity and specificity of chest radiography for the detection of lung cancer are 78.3% and 97.0%, respectively [8], whereas for LDCT the sensitivity and specificity are 87.7% and 99.3%, respectively [2]. Chest radiography only detects lung cancer in ∼77–80% of cases in the year before diagnosis [9]. Therefore, LDCT is used as the primary method of cancer screening, and CT is subsequently performed if abnormalities are detected on chest radiographs.

Solitary pulmonary nodules (SPNs) are increasingly detected with the widespread use of chest radiography and chest CT scans. According to the National Institute for Health and Care Excellence (NICE) guidance, chest radiography is recommended for several symptoms in patients aged >40 years [10]. Findings on chest radiography that are suspicious for lung cancer warrant an urgent referral within 28 days, and additional workup [10].

TABLE 1 Comparison of conventional and digital chest radiography

	Conventional	Digital
Examination time	Longer; film development required	Shorter; can be viewed immediately; no film development required
Post-processing manipulation (*e.g.* magnification, windowing, greyscale inversion)	Not possible	Possible; in the case of under- or over-exposed film, they do not need to be repeated, so the patient's radiation exposure is also reduced
Graphic quality	Lower	Higher
Storage	Storage space is required; chemicals and films are highly polluting	Completed films can be stored digitally, which can be viewed simultaneously and remotely
Interpretation time	Prolonged	Shorter
Price	More expensive	Cheaper
Accessibility	More complicated	Easier

The "blind zones" on postero-anterior chest radiographs (apices, hila, retro-cardiac and sub-diaphragmatic spaces) and the mediastinal lines and stripes (lines) should always be checked carefully, since subtle parenchymal nodules can be overlooked here due to overlying and distracting anatomical structures (figure 1). Computer-aided diagnosis (CAD) chest radiography and AI-based software have improved the detection of actionable lung nodules on chest radiographs [11, 12]. The management of patients with SPNs must include estimation of the probability of cancer-suspicious lesions, based on the patient's clinical risk factors and CT characteristics.

Lung tumours may present as central or peripheral masses. The central neoplasm may have hilar lymph node enlargement, mediastinal invasion or bronchial obstruction, with partial or total lung collapse; a parenchymal consolidation or super-infection may exist, which may mask or be the first sign of a possible underlying neoplasm. Retrospective comparison with previous chest radiographs is helpful to determine if a lesion has changed its size and appearance. Unchanged size for 2 years is a sign of benignity.

Prior to CT imaging, chest radiography may play roles in assessing lesion size and demonstrating features of local (for instance bony) invasion, as well as assessing post-obstructive collapse and pleural effusion. Chest radiography can demonstrate obvious chest wall and mediastinal invasion in large tumours; however, it has a limited sensitivity to predict T3 and T4 disease [13]. Accordingly, chest radiography cannot detect invasion of the chest wall, diaphragm or mediastinum, or nodal involvement [14].

Limitations of chest radiography must be emphasised. 45–81% of missed lung cancers occurred in the upper parts of the lung [15]. The detection rate is 29% for tumours measuring a diameter ⩽10 mm [16]. A 2019 review of 21 studies reported that 20–23% of chest radiographs in patients with lung cancer symptoms were falsely negative for lung cancer [9].

In summary, chest radiography remains the first-line investigation for lung cancer in primary care and the most common radiological route to diagnosis. NICE lung cancer guidelines recommend chest radiography for initial evaluation in all patients, aside from those aged >40 years who have unexplained haemoptysis [10].

The role of CT in diagnosis and follow-up

CT is the most important imaging modality in the imaging of lung cancer. When the chest radiograph raises the suspicion for malignancy, CT with contrast should be performed for complete staging. Administration of intravenous contrast is necessary for the evaluation of contrast enhancement in the lesion, and for the better differentiation of the surrounding tissues (*e.g.* in the case of atelectasis), mediastinal and hilar regions, especially the lymph nodes. Multidetector CT (MDCT) scanners are capable of examining the whole lung within a single breath-hold, which increases the accuracy of the contrast material administration. Additionally, MDCT takes thin slices, which improves the spatial resolution of

FIGURE 1 Images of a 73-year-old female patient admitted to hospital for secondary hypertension workup and management. a) A routine chest radiograph showed a right basal pulmonary nodule, which was misdiagnosed as the right nipple, but b) computed tomography (CT) and c) CT-guided biopsy confirmed the presence of a carcinoid tumour. In addition, a) chest radiography and CT (not shown) confirmed an aberrant right subclavian artery, known clinically as arteria lusoria, which is the most common embryological abnormality of the aortic arch. Images courtesy of the Medical Imaging Centre, Semmelweis University, Budapest, Hungary.

multiplanar reconstruction images and increases the quality of maximum intensity projection images and 3-dimensional (3D) reconstructions [2]. The CT parameters are most commonly 120 kVp, 20–80 mAs and 3–5-mm slice thickness.

64-slice to 128-slice CT scanners generally offer shorter examination time than the previous systems, such as 16-slice CT scanners (table 2), which further increases the advantages of MDCT, for example by reducing motion artefacts [17]. The comparison of dose efficiency of scanners with different numbers of slices is an interesting question in the dosimetry of radiology. A study compared 4-, 8-, 16- and 64-slice scanners by measuring dose in anthropomorphic phantoms: they concluded that the organ dose in the middle of the scan was the same, while organs at the ends of the scan received a higher dose in the case of the 64-slice scanner, because of the larger over-ranging [18]. Another study compared a prototype 256-slice scanner with a 16-slice commercial CT: in the case of a chest examination they found that the 256-slice scanner used only 72.1% of the dose used by the traditional one [19]. A third study found that MDCT with a larger number of slices uses a higher dose but delivers better image quality scores in the case of chest examinations [20]. Several international radiology societies have published guidelines on the CT requirements for lung cancer screening; for example, the American College of Radiology (ACR) recommends using at least 16-slice MDCT, whereas the European Society of Thoracic Imaging (ESTI) sets the lower limit at 32-slice and recommends 64-slice MDCT [21].

The slice thickness, considering the radiation dose, is 1.0-mm slice thickness or smaller, with the LDCT protocol for lung cancer screening [22]. For lung cancer staging and pulmonary nodule assessment, thin-section axial chest CT data with slice thickness of 1–1.25 mm are recommended [23–26]. This slice count category is a bit more expensive than those with a lower number of slices.

According to the Fleischner Society's recommendations, initial CT for the assessment of SPNs should be intravenously contrast enhanced to exclude additional intrathoracic abnormalities, and subsequent surveillance CT scans should be non-contrast, thin section and ideally low radiation dose when follow-up of a pulmonary nodule is the only indication for CT [27, 28]. Intravenous contrast administration helps to differentiate the tumour from the surrounding atelectasis and to characterise the necrotic parts of the cancer.

Multiplanar reconstructions create multiplanar reformation images of the malignancy, making the assessment of its relationship to surrounding structures (including fissures and the diaphragm) possible [2, 29]. Maximum intensity projection images increase the detection rate of small pulmonary nodules, especially in the central lung areas, which helps to reduce the number of overlooked small cancers [2, 30]. 3D reconstructions also help the assessment of the lung cancer [2, 31] by improving spatial orientation and can identify surgically relevant structures and their interindividual variance [32]. Virtual bronchoscopy, a CT-based internal 3D rendering technique of the airways, allows a noninvasive intraluminal evaluation of the tracheobronchial tree for the evaluation of cancer-related airway stenosis [2].

The CT scan of the primary lung cancer may demonstrate a wide spectrum of appearances. Nonsmall cell lung cancers (NSCLCs) can be either centrally or peripherally located masses, invading the mediastinal structures and the chest wall, which usually demonstrate a solid appearance as a solitary nodule or a consolidation-like mass (>3 cm) [13]. Tumour margins can be smooth, lobulated, irregular and spiculated. Squamous cell carcinomas tend to be centrally located, might contain central necrosis or cavitation, and are associated with post-obstruction atelectasis, inflammation and infection. Adenocarcinomas, usually the *in situ* forms, tend to have a peripheral location; therefore, these lesions are associated with less obstruction, inflammation and necrosis, and usually demonstrate a ground-glass or part-solid appearance (figure 2) [33]. Larger adenocarcinomas may demonstrate a consolidation with air bronchogram. Small cell lung cancers are often centrally located, show a rapid growth with invasion of the mediastinal and hilar structures, causing

TABLE 2 Differences in imaging duration and radiation dose between chest computed tomography scanner types

	16-slice	64-slice	128-slice
Imaging duration (s)	~8.3	~8.5	~3.5
Effective dose (mSv)	9.52	7.5	9.46
$CTDI_{vol}$ (mGy per 100 mAs body)	11.65	17.11	10.4±2.1

Note that these are example values, since different studies have reached different results regarding the dose efficiency of multislice computed tomography scans. $CTDI_{vol}$: volume computed tomography dose index.

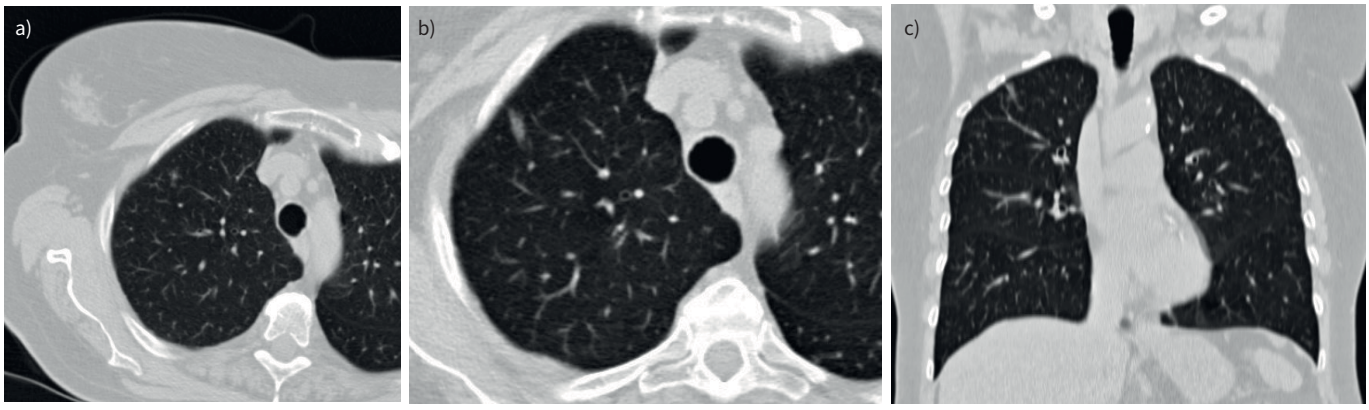

FIGURE 2 Computed tomography (CT) scans of a growing part-solid nodule. a) In 2014. b) Axial and c) coronal views from 3 years later, in 2017. The 70-year-old female smoker patient was investigated due to cough. Positron emission tomography/CT did not show fluorodeoxyglucose uptake in the lesion. Biopsy confirmed adenocarcinoma. Images courtesy of the Medical Imaging Centre, Semmelweis University, Budapest, Hungary.

bronchial stenosis/obstruction and nodal involvement [34]. Most cases of peripheral small cell lung cancer manifest as a lobulated mass rather than a spiculated mass [34]. Finally, carcinoid tumours usually appear as a solid, lobulated nodule [35].

Malignant SPNs have been shown to have significantly higher mean attenuations of enhancement (<15 Hounsfield units (HU): benign; >15 HU: malignant) and higher washout on a 15-min delay series than all benign SPNs [36]. Nodule detection can be improved by CAD and AI-based programs, especially for centrally located nodules compared to peripheral ones [37, 38]. In cases of suspected lung cancer, bronchoscopic or image-guided biopsy is necessary to obtain histological diagnosis [13].

For staging, currently the eighth edition of the TNM classification for lung cancer staging is recommended by the International Association for the Study of Lung Cancer (IASLC) [39]. In recent years, new patient data have been collected to develop the ninth edition, which is expected to be completed in 2024 [40, 41]. Briefly, the analysis of the T component is based on the tumour size, endobronchial location, atelectasis/pneumonitis, and invasion of the diaphragm [41]. Tumour size must be measured on lung window images without measuring the spiculations [23, 27]. For part-solid nodules, suggestive of adenocarcinoma, measuring size involves measuring the longest diameter of the solid part, as well as the non-solid part beyond it on the CT scan, to determine the overall size of the tumour [23]. CT scans play an important role in T-staging, including showing proximity of the tumour to the main pulmonary artery or its involvement, involvement of the fissures, endobronchial tumour involvement and its distance from the carina, invasion of the chest wall, and invasion (lysis/destruction or definite sclerosis) of ribs and chest wall musculature as well as the mediastinum [13]. Moreover, CT with intravenous contrast is essential in N- and M-staging. Mediastinal and hilar nodal disease is evaluated using CT scans with intravenous contrast and, more recently, PET/CT has been used for its evaluation, due to its higher sensitivity and specificity [13]. A lymph node with short axis diameter of >1 cm is generally considered to be malignant. However, metastatic lymph nodes (usually between 4 and 10 mm) can be more sensitively analysed with PET/CT than with CT [42].

Intra- and extrathoracic metastases can be detected on CT scans with a degree of certainty, including pleural and pericardial effusions and metastatic lung nodules. Adrenal and liver metastases are common in lung cancer; therefore, it is recommended that the scan coverage should include the upper abdomen [13].

Follow-up CT scans help in the monitoring of the response to treatment, in the detection of recurrent tumours and in the planning of radiation therapy [2]. During the follow-up of treated/resected NSCLC patients, the use of thoracic CT scans enables the detection of more cases of early recurrence and second primary lung cancer, which are more amenable to curative-intent treatment, according to the IFCT-0302 study, a prospective randomised trial, which is a major study and the largest in this field [43].

In recent decades, tremendous improvements in scan speed, volume coverage, spatial and soft tissue resolution and dose reduction have been achieved, mainly involving tube current modulation, automated exposure control, anatomy-based tube voltage (kV) selection, advanced X-ray beam filtration, and iterative image

reconstruction techniques, which improved image quality and decreased radiation exposure [44]. The emergence of MDCT and use of advanced iterative reconstruction algorithms have enabled volumetric lung images to be achieved at high spatial resolution and low radiation doses. In addition, AI is increasingly used in patient positioning, protocol adjustment, image reconstruction, image pre-processing or post-processing [44].

In 2021, the first clinical photon-counting detector system, referred to as photon-counting CT (PCCT), was approved, which provides ultrahigh resolution (0.2 mm and 0.4 mm) images and is considered an innovation in CT technology [45, 46]. PCCT relies on the direct conversion of incoming photons into electrical charges that are subsequently transferred into a current that is proportional to the energy of the incoming photons (energy-integrated detectors). Due to the absence of electronic noise, improved radiation dose efficiency, increased iodine signal, lower doses of iodinated contrast material administration, and better spatial resolution can be achieved. In addition, spectral imaging can be performed and quantitative functional data such as lung perfusion data can be obtained [47]. PCCT also allows K-edge imaging, which, combined with new contrast materials specifically designed for PCCT, opens the door to new applications for imaging in the future [47].

The role of MRI in diagnosis and follow-up

MRI of the chest is still considered a supplementary imaging tool in cases of lung cancer, used for the determination of tumour invasion in the chest wall and the mediastinal structures (especially in cases of pancoast tumour), differentiation between solid and vascular hilar masses (using ECG-triggered magnetic resonance angiography to reduce cardiac motion- and breathing-related artefacts in pulmonary vessels), assessment of diaphragmatic abnormalities and in cases of mediastinal lymphoma (table 3) [2].

It is not possible using MRI to assess the airway and lung parenchyma, due to low proton density and artefacts due to respiratory and cardiac motion [48]. However, with recent advances related to MRI pulse sequences, post-processing software and analysis methods, multi-coil parallel imaging and acceleration methods, and the administration of contrast media, pulmonary MRI has become a considerable imaging modality in lung cancer [49, 50]. On the one hand, higher lesion contrast can be expected at 3 T compared to 1.5 T machines [49]. On the other hand, the performance of low-field (0.55 T) MRI systems equipped with high-performance image technology can reduce distortion by reducing susceptibility and deliver excellent image quality because of improved field homogeneity (figure 3) [49, 51]. Due to their lack of signal, the blood vessels are well separated from the soft tissues and tumours. Therefore, MRI is more sensitive in terms of vascular infiltration.

Whole-body MRI may detect distant metastatic disease [2, 52]. Diffusion weighted imaging (DWI) is a powerful imaging tool that provides unique information related to tumour cellularity and the integrity of the cellular membrane; therefore, it can be applied for tumour detection, characterisation of different subtypes (based on ADC values) and N- and M-stage evaluation, as well as for the monitoring of response to treatment [2, 53, 54]. Dynamic contrast-enhanced (DCE) MRI indexes can differentiate potentially malignant and benign SPNs [55].

Several studies have demonstrated that lung MRI could be a potentially effective screening tool, with a performance comparable to that of LDCT, but with a lower false-positive rate and no radiation exposure

TABLE 3 Indications for magnetic resonance imaging (MRI) in the context of lung cancer diagnosis and follow-up

Role in diagnosis and staging	Role in follow-up
Determination of tumour invasion in the chest wall and the mediastinal structures	Monitoring of response to treatment
Differentiation between solid and vascular hilar masses	N- and M-stage evaluation, *e.g.* screening for brain, vertebral/spine metastases
Assessment of tumour cellularity	Assessment of diaphragmatic abnormalities during treatment
Characterisation of different subtypes	Assessment of distant metastatic disease (whole-body MRI)
N- and M-stage evaluation, *e.g.* screening for brain, vertebral/spine metastasis	
Assessment of distant metastatic disease (whole-body MRI)	
Assessment of diaphragmatic abnormalities	
Differentiation of lung cancer from progressive massive fibrosis, tuberculomas, obstructive pneumonia and surrounding post-obstructive atelectasis	

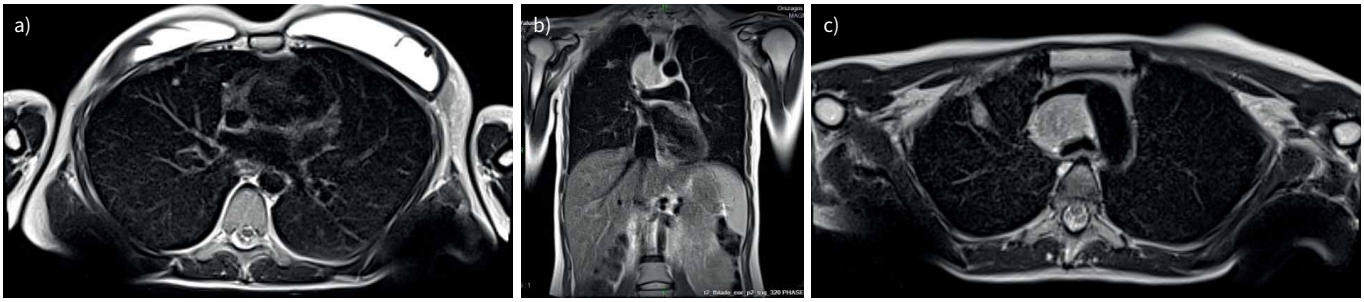

FIGURE 3 Low-field magnetic resonance imaging (0.55 T) images (T2 FBLADE sequence). a) Axial and b) coronal views of a metastatic lung nodule in the right upper lobe (S3 segment), and c) axial view of another metastatic pulmonary lesion in the right upper lobe and a growing mediastinal lymph node, in a young female pregnant patient with metastatic breast cancer. Images courtesy of the National Institute of Oncology, Budapest, Hungary.

[49, 56]. MRI can differentiate lung cancer from progressive massive fibrosis, tuberculomas and obstructive pneumonia as well as from surrounding post-obstructive atelectasis [49]. In addition, MRI has a high diagnostic performance for N-staging in NSCLC using short tau inversion recovery (STIR) turbo-spin echo (TSE) sequence and DWI [57, 58], and screening for brain metastases by contrast-enhanced MRI is useful in patients with clinical stage III lung cancer considered for curative therapy [59].

Recently, various MRI techniques, for instance 3D DCE-perfusion sequence, have been shown to be useful in the prediction of post-operative lung function in lung cancer patients with underlying COPD [49, 60]. Additionally, magnetic resonance lymphangiography has been shown to be promising in the detection of post-operative chylothorax after pneumonectomy and lobectomy [49]. Finally, MRI might play a role in treatment response evaluation with DWI sequence, such as in differentiating between radiation pneumonitis and true progression [49, 61].

Despite the developments in MRI technique described here, access to MRI is a major issue for patients and clinicians even in European countries, greatly restraining its involvement in lung cancer patient management except in specific cases such as lung apex cancer, involvement of vertebra (and spine), or brain MRI for staging.

The role of nuclear medicine in diagnosis and follow-up

Nuclear imaging techniques visualise molecular processes *in vivo*. Together with radiological imaging, multimodal functional and morphological imaging addresses two main topics in respiratory medicine: the individualised workup of lung cancer and pulmonary thromboembolic diseases. In lung cancer, PET with integrated CT currently serves as a first-line staging tool, provides essential information for radiotherapy planning, and monitors response to therapy [62–64].

An integral part of nuclear medical imaging is the radiotracer, which consists of a chemical compound and a radionuclide. Since malignant tumours in particular express glucose transporters (GLUT 1 and 3) on their outer cell membranes, glucose serves routinely as a suitable chemical compound in proliferating cells. Increased glucose uptake is based on the Warburg effect, describing that proliferating neoplastic cells increasingly use cytoplasmic glycolysis for nucleic acid and lipid biosynthesis instead of mitochondrial glucose oxidation, despite the presence of oxygen [65]. Labelling with the positron emitter fluorine-18 (^{18}F) produces fluorodeoxyglucose (FDG), which is used as a radiotracer for temporal and spatial imaging of glucose metabolism. FDG cannot be further metabolised after phosphorylation and accumulates especially in tumour tissue (known as “metabolic trapping”). The semi-quantitative assessment of cellular FDG uptake from a target region is usually carried out by calculating the standardised uptake value (SUV), measuring the uptake in a tumour normalised to the distribution volume. An SUV mean cutoff >2.5 has been used to differentiate between benign and malignant nodules [66]. However, other factors, such as the time of SUV evaluation, the shape of the region of interest (ROI), attenuation correction and body size, influence the calculation of SUV [67]. In addition, the SUV is also influenced by biological factors of the pulmonary nodules, *e.g.* slowly growing and well-differentiated tumours generally have lower SUVs than rapidly growing and undifferentiated ones [68]. Differential diagnoses of FDG uptake by means of PET/CT have an impact on further workup, which is why knowledge of false-positive and false-negative findings is essential. Table 4 gives an overview of the differential diagnoses of cellular FDG uptake.

https://doi.org/10.1183/20734735.0176-2023

TABLE 4 Differential diagnoses of cellular fluorine-18 (^{18}F) fluorodeoxyglucose (FDG) uptake during tumour staging

Anatomical region	Physiological, norm variant	False-positive ^{18}F-FDG uptake	False-negative ^{18}F-FDG uptake
General	BAT Brain Myocardium Kidneys Urinary tract	Inflammation Area of surgery Iodinated contrast medium Incorrect alignment (fusion) of PET and CT Incorrect attenuation correction	Hyperglycaemia Small tumours Low ^{18}F-FDG avidity Regions of low physiological ^{18}F-FDG uptake Incorrect alignment (fusion) of PET and CT Incorrect attenuation correction
Head and neck	Brain: white and grey matter Neck: neck muscles and BAT, *e.g.* supraclavicular	Head: Sinusitis Neck: Thyroiditis Graves disease Warthin tumour Reactive lymphadenopathy	Intracranial metastasis Glioma, low-grade
Thorax	Thymus Oesophagus BAT: mediastinal, pericardial, paravertebral, intercostal Myocardium Autochthone muscles Lactating breasts	Sclerosis of the aorta Oesophagitis Pleural empyema Pleurodesis Pneumonia, abscess Radiation pneumonitis Granulomatosis: mycobacteria, sarcoidosis, aspergillosis, arteritis Reactive mediastinal lymphadenopathy (including sarcoid-like lesion) Thymus rebound following chemotherapy Mastitis, gynaecomastia Metal implants	Lung: Lepidic adenocarcinoma Carcinoids Solitary pulmonary nodules <8 mm
Abdomen	Stomach, intestine Liver, spleen Kidneys, ureter, urinary bladder BAT: perirenal	Adrenocortical hyperplasia Vascular bypass Polyp and adenoma Pancreatitis	MALT lymphoma Hepatocellular carcinoma Renal cell carcinoma
Bones, joints	Skeletal musculature	Reactive bone marrow stimulation due to G-CSF Bone marrow stimulation (anaemia, post-chemotherapy) Inflammation, infection: arthritis, phlebitis, spondylodiscitis, osteomyelitis Fibrous dysplasia Paget disease of the bone Bone cyst	Radiation of the bones Chondrosarcoma Solitary plasmacytoma of bone Sclerotic metastases

BAT: brown adipose tissue; PET: positron emission tomography; CT: computed tomography; MALT: mucosa-associated lymphoid tissue; G-CSF: granulocyte colony-stimulating factor. Information from [69, 70].

False-positive findings have been reported in infectious diseases (mycobacterial, fungal and bacterial infection), sarcoidosis, radiation pneumonitis and post-operative surgical conditions, while tumours with low glycolytic activity such as adenomas, low-grade and *in situ* adenocarcinomas, carcinoid tumours, low-grade lymphomas and small-sized tumours (SPNs <8 mm) have revealed false-negative findings on PET scans [71]. Immune checkpoint inhibitors can upregulate the immune pathways, resulting in a wide variety of adverse effects, such as reactive adenopathy with increased FDG uptake. In addition, pseudoprogression has been identified in melanoma patients receiving ipilimumab therapy. Therefore, utilisation of iRECIST guidelines (Response Evaluation Criteria in Solid Tumours in cancer Immunotherapy trials) when reporting studies that demonstrate possible progression, and careful review of all components of the PET/CT, prior imaging and the patient's clinical history, are essential to avoid misinterpretation [72]. Moreover, SUV, which is normalised for body weight, overestimates metabolic activity, and this overestimation is more significant in obese patients than in patients with a normal body mass index. In this respect, SUV normalised by lean body mass is not affected by body weight and appears to produce more accurate SUV results [73].

In clinical routine, the basic workup of suspicious pulmonary nodules or masses should include contrast-enhanced CT of the thorax and the abdominal region. CT visualises localisation and radiological characteristics of suspicious morphology and assesses the therapeutic effect of treatment [74, 75]. However, information about tumour vitality and metabolism as well as on the mediastinal lymph nodes is not sufficiently provided with CT as the diagnostic tool. Multimodal FDG-PET/CT makes it possible to co-register glucose metabolism (as a surrogate parameter for tumour vitality of a nodule suspicious for lung cancer) together with morphology [69]. The T descriptor is usually reliably detected by CT, including accurate determination of the maximum longitudinal diameter of the target lesion and infiltration of pleura, vessels, mediastinum, bone or pericardium. Hybrid FDG-PET/CT uses imaging of metabolic tumour extension to better estimate infiltration into surrounding tissues, metabolically active pleural effusion, and tumour size in atelectasis, than is possible with CT alone (figure 4). PET/CT is also superior to CT alone in sensitivity and specificity for determining the N descriptor, and can guide the histological workup of mediastinal lymph nodes suspicious for malignancy by endobronchial ultrasound (EBUS) or video-assisted mediastinoscopy.

FDG-PET/CT provides helpful information about both thoracic (local) and extrathoracic (distant metastatic) lesions. The detection of extrathoracic lymph node metastases, adrenal, bone and bone marrow metastases on PET/CT can guide further tissue workup (such as image-guided biopsy). During radiotherapy planning, FDG-PET complements CT imaging to narrow down the radiation volumes of hypermetabolic tumour

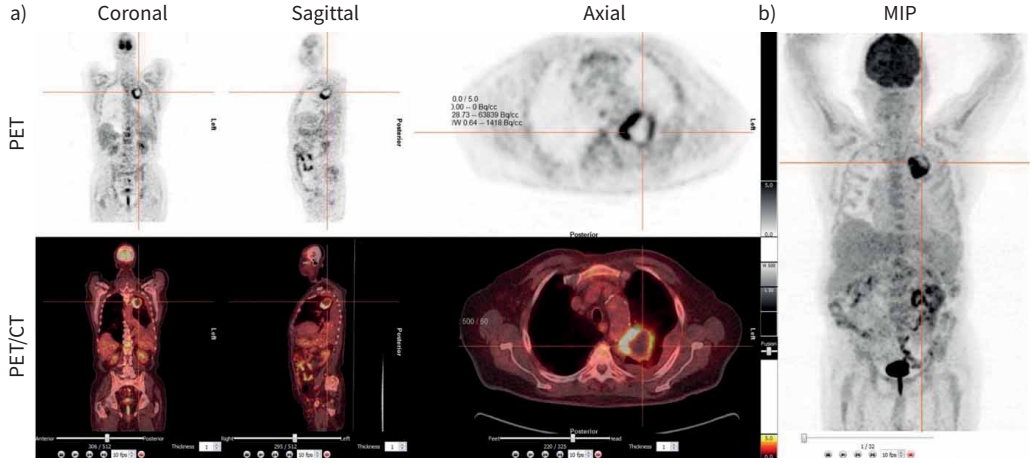

FIGURE 4 a) A fluorine-18 fluorodeoxyglucose (^{18}F-FDG) positron emission tomography (PET)/computed tomography (CT) image in three sectional planes of an 82-year-old smoker. In the left upper lobe, a pulmonary mass with a hypermetabolic border (maximum standardised uptake value 13.6) and a necrotic centre comes into view. Staging remained without evidence of mediastinal or extrathoracic metastasis. b) The maximum intensity projection (MIP) shows an overview of the entire PET scan. Information about the distribution of FDG uptake assisted CT-guided puncture, which was taken from the marginal area of the pulmonary mass and confirmed a pulmonary squamous cell carcinoma.

tissue (*e.g.* mediastinal lymph nodes). PET is also suitable for assessing therapy response by showing metabolic activity in the target lesions after local (radiotherapy) and/or systemic therapy. In addition, it is used during multidisciplinary team discussion to assess the course of suspicious CT findings in terms of progress or recurrence of disease [76].

PET tracers other than ^{18}F-FDG may play a potential role in imaging tumour biology and heterogeneity by assessing hypoxia, proliferation, and vasculature. Neuroendocrine tumours of the lung, such as carcinoids, large cell neuroendocrine and small cell carcinomas, show both neuroendocrine morphology (organoid or palisade-like structures) and neuroendocrine differentiation (chromogranin A, synaptophysin, *etc.*), depending on the degree of differentiation. They can express membrane-bound somatostatin receptors (SSTRs) 1–5 on the cell surface, which indicate the presence of a neuroendocrine tumour in tumour-specific structures. For staging of neuroendocrine tumours, assessment of SSTRs by means of gallium-68 (^{68}Ga) dodecane tetraacetic acid (DOTA) scan is an appropriate imaging modality [77]. Here, DOTA acts as a complexing (chelating) agent for the radionuclide ^{68}Ga. ^{68}Ga-DOTA complex is conjugated with peptides, such as octreotide and octreotate (DOTATOC or DOTATATE, respectively). These ^{68}Ga-DOTA-conjugated peptides are used as tracers in PET/CT imaging for the identification of neuroendocrine tumours and quantification of specific tumour metabolism. Figure 5 depicts a case study in which SSTR-specific tracers and PET/CT imaging were applied for the diagnosis of a neuroendocrine tumour of the lung.

The most commonly used hypoxia tracers are ^{18}F-FMISO (fluoromisonidazole), ^{18}F-HX4 (flortanidazole) and ^{18}F-FAZA (fluoroazomycin arabinoside). ^{18}F-FLT (fluorothymidine) can be used to study proliferation. Because hypoxia is a marker of radioresistance and areas of high proliferation, which are presumably more aggressive, such tumour areas may require dose escalation [78–85]. A prospective, phase II multicentre dose escalation study using ^{18}F-FMISO in NSCLC patients showed the feasibility of increasing the dose up to 86 Gy in hypoxic subvolumes. After 3 years of follow-up, the authors found that in ^{18}F-FMISO-positive patients, radiation therapy escalation increased median overall survival by 11.2 months [86, 87].

Using ^{68}Ga-pentixafor PET/CT, it is possible to quantify the CXCR4 receptor *in vivo* in different lung cancer subtypes, as well as to examine the correlation of quantity of CXCR4 receptors with tissue density by immunochemical analyses. ^{68}Ga-pentixafor PET/CT proved to be highly sensitive and specific for *in vivo* targeting of CXCR4 receptors in lung cancer, so it can be effectively used to assess response and develop CXCR4-based radioligand therapies [88].

In conclusion, results from nuclear imaging techniques give critical direction to prognosis and treatment planning. A multimodal nuclear medical imaging technique, PET/CT forms a mainstay in the workup of thoracic tumour diseases and makes an important contribution to individualised therapy in patients with lung cancer.

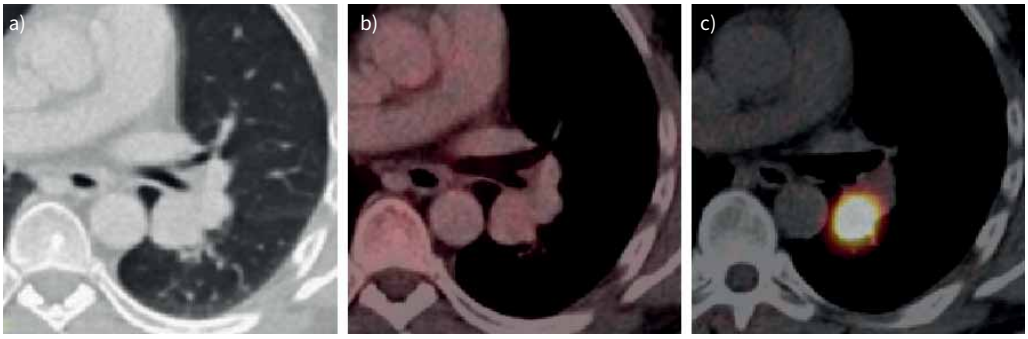

FIGURE 5 Positron emission tomography (PET)/computed tomography (CT) of a 56-year-old smoker who presented with a chronic dry cough. In the left lower lobe of the lung, a) CT showed a solid compaction (23 mm) close to the hilus, which in b) fluorine-18 fluorodeoxyglucose (^{18}F-FDG) PET/CT showed only a slightly increased uptake (maximum standardised uptake value (SUV_{max}) 3.2) and was not considered to be malignant. c) Somatostatin receptor expression was significantly increased in the gallium-68 dodecane tetraacetic acid-conjugated octreotide (^{68}Ga-DOTATOC) PET/CT at this site (SUV_{max} 43). Left lower lobe resection revealed a typical carcinoid.

Lung cancer screening

Throughout Europe, LDCT screening for lung cancer is in a phase of clinical implementation. In the USA, the National Lung Screening Trial demonstrated that LDCT screening leads to a 20% reduction in lung cancer-associated mortality in high-risk populations compared to that seen with chest radiography [89]. The US Preventive Services Task Force recommends annual screening for lung cancer with LDCT in adults aged 50–80 years who have a 20-pack-year smoking history and currently smoke or have quit within the past 15 years [90]. LDCT for lung cancer screening in high-risk subjects has started to be used in routine clinical practice in some countries, since LDCT screening may facilitate early diagnosis and thus curative-intent treatment in lung cancer (figure 6) [91]. The LDCT-based Lung CT Screening Reporting and Data System (Lung-RADS) is widely used for nodule assessment and subsequent management [92].

The drawbacks of LDCT screening include the number of unnecessary invasive procedures or complications due to the high malignancy-related false-positive rate (23%) [89], which can be decreased by appropriate nodule classification using deep learning methods and radiomics [3, 93]. The longer-term COSMOS study demonstrated an intermediate benefit-to-radiation-risk ratio of approximately 23:1, assuming 20% mortality benefit [94]. In LDCT trials, volume CT dose index ranged from 0.8 to 3.81 mGy depending on the participant's body weight, with an average effective dose estimate of ⩽2 mSv per CT [95]. The sensitivity and specificity of LDCT, in successfully diagnosing early-stage lung cancers were 87.7% and 99.3%, respectively [2].

The American College of Radiology Appropriateness Criteria have been recently updated, with publication in November 2023, reviewing the available literature on various imaging modalities and summarising management of incidentally detected indeterminate pulmonary nodules [96]. In the past decade, ultra-low-dose CT (ULDCT) has been gaining more attention, offering a sub-millisievert radiation dose (approximately equal to two chest radiography sessions) [97]. Although limitations, such as lack of former human experiences, hamper the comprehensive understanding of technology applicability to the clinical setting, ULDCT by spectral shaping seems a promising technique for the detection and characterisation of SPNs, with an excellent agreement with LDCT, as well as a feasible approach for lung cancer screening [98]. However, the role of ULDCT in the diagnosis and workup remains unsolved. The latest articles suggest that ULDCT can be utilised for screening and follow-up studies of primary or secondary lung cancers for the detection or exclusion of solid pulmonary nodules of size >3 mm and monitoring of the number of >3-mm-sized solid pulmonary nodules [99].

Pulmonary nodules and their management

In chest imaging, a pulmonary nodule is defined as a rounded or oval opacity measuring <3 cm in diameter. Small pulmonary nodules are defined as lesions <8 mm in diameter, while micronodules are diagnosed if the diameter is <3 mm [100, 101]. Pulmonary nodules can be classified, according to their composition, as solid or sub-solid. Sub-solid nodules can be subdivided into pure ground-glass opacities or

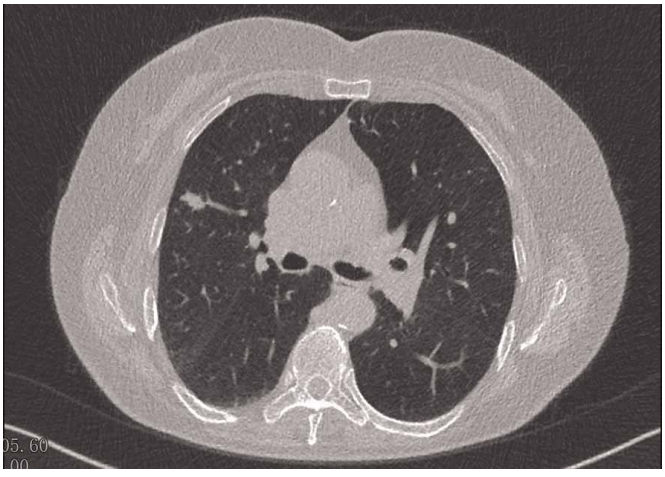

FIGURE 6 Low-dose computed tomography screening of a 77-year-old female smoker, which confirmed a tumour-suspicious speculated solid lesion in the right upper lobe. Image courtesy of the National Institute of Oncology, Budapest, Hungary.

part-solid lesions that contain both ground-glass and soft tissue elements. Pulmonary nodules are commonly found during routine radiological examinations or during lung cancer screening with LDCT scanning. They are identified in 0.2–2% of chest radiographs and in 10–40% of CT scans [101–104]. The prevalence of malignancies among pulmonary nodules diagnosed during lung cancer screening programmes is about 0.5–3.5% [101, 102].

The differential diagnosis of pulmonary nodules includes neoplasms (benign or malignant) and lesions caused by infection, inflammation, vascular abnormalities or congenital malformations. The majority of pulmonary nodules are benign; however, a few can be malignant. Differentiation of pulmonary nodule character is an important clinical problem, as malignant nodules need to be removed without delay while benign lesions only need to be monitored [101–104].

Chest imaging and clinical characteristics of the patient are key factors in predicting the probability of malignancy in pulmonary nodules. The most frequent independent clinical predictors of pulmonary nodule malignancy are older age and relevant smoking history. Chest CT without contrast is the most appropriate imaging tool in the evaluation of incidentally detected indeterminate pulmonary nodules identified on chest radiographs or CT [96]. Radiological features associated with increased risk of malignancy in pulmonary nodules include large nodule diameter and volume, spiculated margins, upper lobe location and increase in diameter or volume during follow-up. Predictors of benign character of pulmonary nodules, in turn, are some calcification patterns (diffuse, central, laminar or popcorn), perifissural or subpleural location and stability of nodule size in follow-up or previous scans [101–104].

There are a few clinical models for predicting the probability of malignant character of pulmonary nodules. Among them, the most commonly used are three models based on clinical and CT characteristics, two of which also use PET with ^{18}F-FDG: the Mayo Clinic, Brock University and Herder models [101, 105]. Comparison of these models is presented in table 5. Separate prediction models are dedicated to pulmonary nodules detected during LDCT (PanCan model, Lung-RADS and National Comprehensive Cancer Network (NCCN) guidelines) [106, 107]. An additional criterion used in these models to assess malignant character of the nodule is the volume doubling time, which is particularly useful in small pulmonary nodules (<8 mm in diameter) [101, 102].

When the character of a pulmonary nodule is indeterminate despite chest CT, additional imaging techniques may help differentiate malignant *versus* benign aetiology. Among them, FDG-PET seems to be the most accurate method, with sensitivity >95% and specificity of 82–85% [101, 102, 108, 109]. For a long time, MRI has not been used for lungs, but recent progress in MRI technology now allows for its implementation in lung imaging, including analysis of pulmonary nodules. In comparison to CT, MRI enables accurate assessment of nodule diameter in those >8 mm [110]. Thus, sometimes MRI may be considered an alternative to CT for follow-up of some lung lesions, especially as it is a radiation-free procedure. Recent developments in MRI sequences for the lung, implementing ultrashort echo time on a

TABLE 5 Comparison of prediction models for malignant character of pulmonary nodules identified by chest computed tomography (CT)

	Brock model	Herder model	Mayo Clinic model
Patient characteristics			
Age	+	+	+
Sex	+		
Smoking history		+	+
Family history of lung cancer	+		
Emphysema	+		
Previous history of extrathoracic cancer		+	+
Nodule characteristics			
Size	+	+	+
Upper lobe location	+	+	+
Type (solid/part-solid/GGO)	+		
Spiculated margins	+	+	+
Nodule count	+		
FDG-PET/CT		+	+

GGO: ground-glass opacity; FDG: fluorodeoxyglucose; PET: positron emission tomography.

3 T system, proved that MRI may reach similar sensitivity and specificity to CT in diagnosing all types of pulmonary nodules (solid, sub-solid and ground-glass), although MRI underestimated pulmonary nodule diameter by approximately 1–2 mm [111].

The management of a pulmonary nodule depends on its type (solid *versus* part-solid *versus* pure ground-glass nodule) and its probability of malignancy. Two algorithms for management are presented in figure 7 [27, 102].

Evaluating complications of treatment in lung cancer

In recent years, immunological checkpoint inhibitors and molecularly targeted drugs have been added to the lung cancer treatment arsenal, in addition to chemotherapy. Immune checkpoint inhibitors are active due to the activation of the immune system to recognise and destroy tumour cells. The most common side-effect associated with immunotherapy is immune-related hypothyroidism (20%). The incidence of other side-effects is much lower: in clinical trials, immune-related adverse events occurred in <5% of patients; the most important among them were pneumonia, inflammatory bowel disease, hepatitis and cardiac toxicities [112]. However, the incidence of pneumonitis among lung cancer patients in daily practice can reach 20% and even 30% in patients after chest radiotherapy, with additional morphological features in this group of patients [113, 114]. Radiological features of pneumonitis are classified into five subtypes: cryptogenic organising pneumonia (19%), ground-glass opacities (37%), interstitial (7%), hypersensitivity (22%) and pneumonitis not otherwise specified (15%) [115]. Pneumonia after immune checkpoint inhibitors is more likely to be bilateral, involving multiple lobes and without sharp borders. In patients who receive both radiotherapy and immune checkpoint inhibitors, lesions may be confined to the lung, with acute borders similar to those seen in radiotherapy-associated pneumonia, or they may be found in a more extensive area [114].

Pulmonary complications are relatively frequent among those taking additional anti-cancer drug treatments, which can be difficult to differentiate from progressive cancer, infection, cardiopulmonary disease and other causes. Radiation therapy can be commonly associated with lung injury (pneumonitis and/or fibrosis) with a strong relationship between radiation dose and volume [116]. The differential diagnosis for pneumonia or lung cancer progression must be based on detailed information from the clinical history. It should be noted that similar interstitial changes can also occur as a complication of treatment with tyrosine kinase inhibitors (brigatinib or osimertinib). They then need to be differentiated, especially as the underlying disease progresses [117].

Radiomics and lung cancer

Radiomics/radiogenomics is an emerging field, reliant on AI to aggregate radiology and genomics data, with the aim of predicting the macroscopic and molecular properties of tissues. In the near future, it is likely to have a major impact on diagnostic and treatment pathways for lung cancer. The pipeline for these biomarkers involves extraction of quantitative imaging features, largely from CT and PET/CT, in order to develop models capable of predicting tumour phenotypes and outcomes [118]. This requires 1) identification and segmentation of a target ROI, *e.g.* a nodule or proven cancer, 2) ROI feature extraction, and 3) association of these characteristics with relevant outputs [119], typically requiring deep learning AI. The ability to predict features that traditionally require invasive sampling has considerable and obvious potential for earlier and more refined personalised treatment. In NSCLC, radiomics have been studied in contexts such as cancer screening, early detection/staging [120], prediction of radiotherapy and immunotherapy response [121, 122] and prognostication [120]. The emerging evidence for neoadjuvant therapies in patients with early-stage NSCLC seems set to accelerate developments in this area further.

Several groups have recently demonstrated successful linkage of radiomic features to genetic and molecular alterations in lung cancer ("radiogenomic biomarkers"). In 2022, Wang *et al.* [123] reported a CT-based model for epidermal growth factor receptor status, with a receiver operator area under the curve (AUC) of 0.748–0.813. Zhang *et al.* [124] and Shao *et al.* [125] independently demonstrated the ability of a similar model to discriminate between a broader range of genotypes, with AUC values >0.85 for both eight- and 10-gene panel features.

Despite this potential, radiogenomic research also faces several challenges, including the need to standardise study methods such as image acquisition and feature extraction protocols. Perhaps the biggest challenge lies in data access and the successful colocation of deidentified imaging, genomic and clinical data with the supercomputing resource needed for deep learning. Given the challenges involved in moving large datasets around, solutions are likely to be cloud-based, mandating creation of trusted research environments with the necessary governance in place. Nevertheless, the potential impact of radiogenomic research on lung cancer practice is considerable.

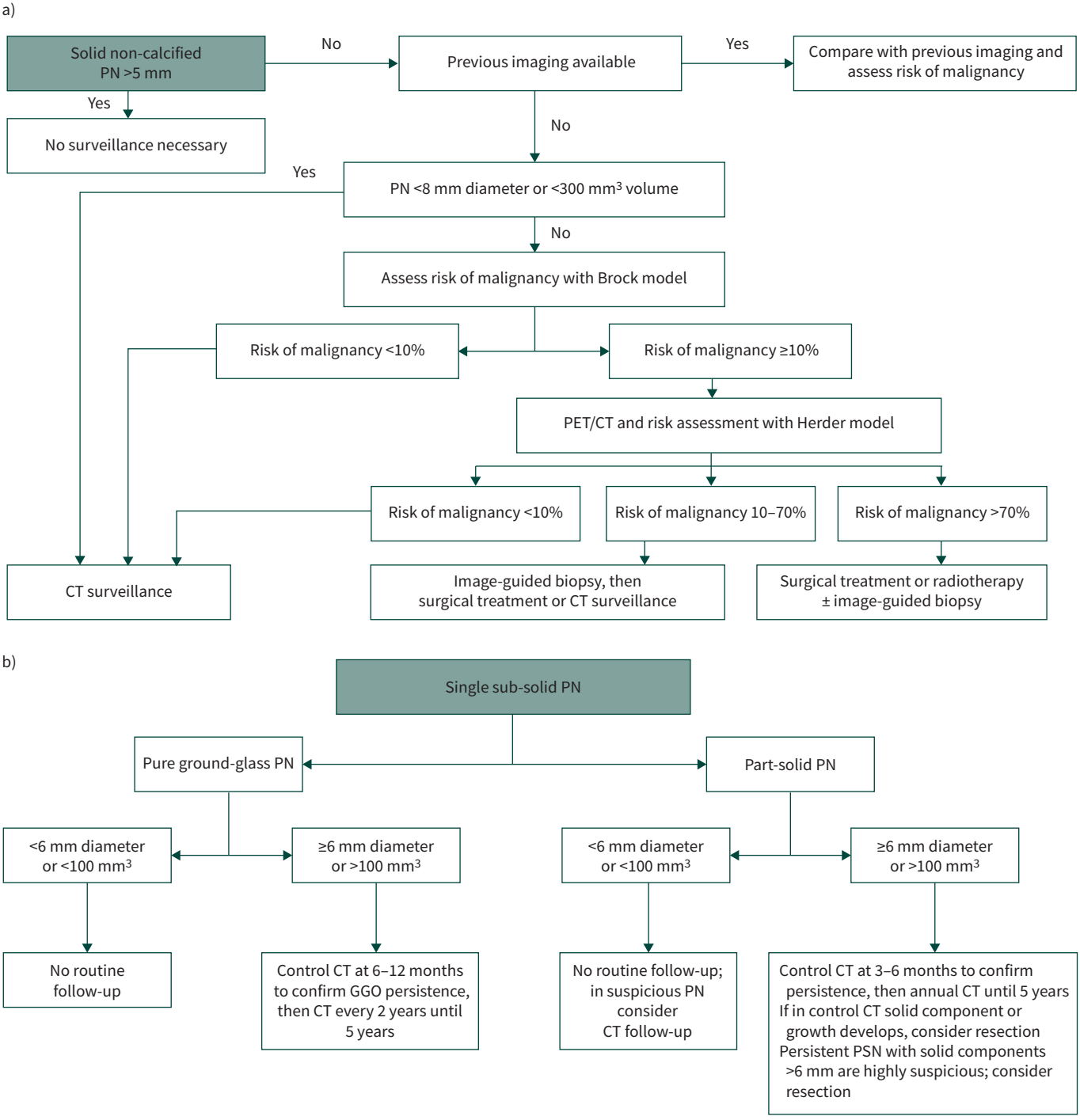

FIGURE 7 a) Algorithm for management of solid pulmonary nodules (PNs) based on British Thoracic Society guidelines. Reproduced and modified from [102] with permission. b) Algorithm for management of sub-solid PNs based on Fleischner Society guidelines. Information from [27]. PET: positron emission tomography; CT: computed tomography; GGO: ground-glass opacity; PSN: part-solid nodules.

Interventional radiology in lung cancer treatment

Ultrasound-guided biopsies

Transthoracic ultrasound-guided biopsies can be used to obtain tissue samples from lung lesions suspected of lung cancer [126]. The procedure holds an excellent diagnostic yield, low complication rate and low costs, and can be performed in an outpatient setting with only local anaesthetics [127]. The methods allow the operator to visualise the needle in the lesions while sampling. However, such methods are only suitable

for lesions visible on ultrasound, and should not be used for lesions without contact to the parietal pleura, lesions inaccessible to ultrasound (such as placement behind the scapula or costae) or lesions with air content (ground-glass opacities). Contrast-enhanced ultrasound can be used to visualise necrotic parts of a tumour and can be used to guide the needle into non-necrotic areas [128].

EBUS is commonly used to stage lung cancer by sampling the hilar and mediastinal lymph nodes [129, 130]. However, the procedure can also be used to sample lung lesions adjacent to the trachea or the main bronchi. Inserting the EBUS scope into the oesophagus allows for tissue sampling of the left adrenal gland, liver, pancreas, lymph nodes below the diaphragm and oesophagus-adjacent lesions [129–134]. Similar to other forms of ultrasound-guided biopsies, sampling is performed with ultrasound visualisation.

CT-guided biopsy

While central lesions in the lung parenchyma and mediastinum suspicious for malignancy are ideally targeted by bronchoscopy or EBUS transbronchial needle aspiration, peripheral pulmonary lesions can be sampled with image-guided assistance (figure 8) [135]. Image-guided biopsy can also help evaluate large mediastinal masses [101]. Image guidance can include ultrasonography or CT. CT-guided transthoracic lung biopsy is performed as needle aspiration or cutting needle biopsy [136]. Both types of CT-guided sampling show greater sensitivity in confirming lung cancer diagnosis than using transthoracic biopsy with fluoroscopy guidance [137]. Direct comparisons between aspiration cytology and cutting needle biopsy in confirming histological diagnosis have revealed that transthoracic needle core biopsy compared with needle aspiration showed similar sensitivity for malignancy (86–98% *versus* 92–98%) [66]. A more recent comparison showed that cutting needle biopsy improved the diagnostic accuracy (98.9% *versus* 93.8%) of pulmonary lesions [138]. Cutting needle biopsy is more likely to yield enough tissue for mutation analysis [101]. This diagnostic advantage for cutting needle biopsy has not been without increased rate of complications, including pneumothorax (20.6% *versus* 13.1%), haemorrhage (32.2% *versus* 13.1%) and haemoptysis (8.2% *versus* 3.3%) [138]. Additional guidance to improve biopsy accuracy can be provided by assessing tumour metabolism through FDG-PET/CT imaging (figure 4).

Emphysema is a predictor of pneumothorax and chest drainage after lung biopsy [139–143]. In addition, forced expiratory volume in 1 s [144] and diffusing capacity of the lung for carbon monoxide [145] have been reported as predictors of pneumothorax, and these should be taken into account when planning and performing biopsy procedures and evaluating risk *versus* benefit for the individual patient. An alternative to CT-guided transthoracic lung biopsy is bronchoscopic tissue sampling, which has a lower risk of bleeding and pneumothorax, allowing for tissue sampling in fragile patients with poor lung function [146]. However, the diagnostic yield for peripheral nodules is considerably lower, even when combined with electromagnetic navigation bronchoscopy [146, 147]. New emerging techniques such as augmented fluoroscopy, cone beam CT and robotic-assisted bronchoscopy may increase the diagnostic yield; however, studies comparing these bronchoscopic modalities to transthoracic CT-guided biopsies are still lacking [148–151].

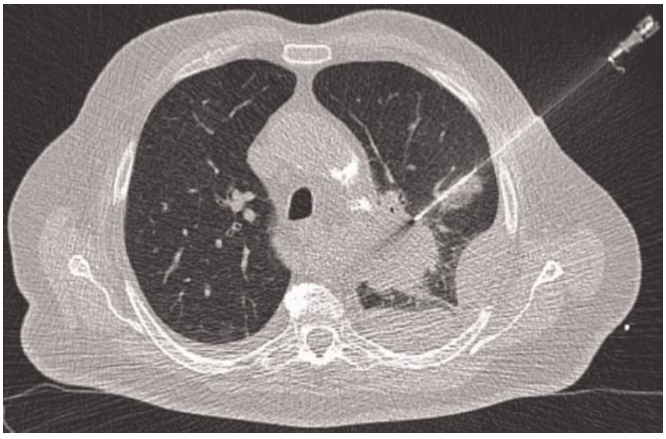

FIGURE 8 Computed tomography (CT)-guided transthoracic lung biopsy performed in the 82-year-old lung cancer patient shown in figure 4. Biopsy location was additionally guided by positron emission tomography/CT. In the case of this central tumour far from the chest wall, bronchoscopic tissue sampling would also have been feasible.

In summary, CT-guided biopsy approaches should be chosen with consideration of the lesion's location and size. These approaches are effective to establish histological diagnosis; however, diagnostic accuracy and incidence of complications may be affected by lesion size or needle path length. The overall complication rate is acceptable, and the major complication rate is low.

Innovative strategies (and trials) using imaging

The intratumoural injection of cytotoxic drugs into endobronchial tumours through a bronchoscope has been described for the treatment of NSCLC and the diagnosis of occult or obvious cancer cell metastasis to mediastinal lymph nodes [152]. Recent clinical trials (phase I to III) conducted on drug delivery systems for lung cancer treatment have investigated targeted therapy and immunotherapy, providing promising directions for personalised treatment [153]. In addition, there is a promising potential capacity of nanomedicine in lung cancer treatment in the future.

Conclusions

Imaging is essential for the management of lung cancer patients. It plays an important role in the screening, detection and staging of disease, and enables characterisation of the radiomic features of the disease, thus guiding choice of the correct therapeutic approach as well as playing a role in the follow-up, post-operative surveillance and treatment response evaluation.

Key points

- Advantages of PCCT include improved radiation dose efficiency, increased iodine signal, lower doses of iodinated contrast material administration, better spatial resolution and spectral imaging, which are all beneficial in lung cancer imaging.
- Through recent advances related to MRI pulse sequences, post-processing software and analysis methods, multi-coil parallel imaging and acceleration methods, and the administration of contrast media, pulmonary MRI has become a considerable imaging modality in lung cancer. Due to its limited accessibility, the involvement of MRI in lung cancer patient management remains restricted to lung apex cancer, involvement of vertebra (and spine) and brain MRI for staging.
- LDCT for lung cancer screening in high-risk subjects is in a phase of clinical implementation in some countries, since LDCT screening may facilitate early diagnosis and thus curative-intent treatment in lung cancer.
- Radiomics/radiogenomics is an emerging field, reliant on AI, which is likely to have a major impact on diagnostic and treatment pathways for lung cancer.

Self-evaluation questions

1. Where has chest radiography a limited sensitivity in lung cancer diagnosis?
2. What are the advantages of PCCT?
3. Where are the current roles of lung MRI in lung cancer imaging?
4. What are the advantages and disadvantages of lung cancer screening with LDCT?
5. What is the role of radiomics/radiogenomics in the diagnostic pathways for lung cancer?
6. Which imaging-guided interventions are available in cases of lung cancer?

Acknowledgements: The authors would like to thank Ákos Sudár (National Institute of Oncology, Budapest, Hungary) for review of the sections about CT doses.

Conflict of interest: Á.D. Tárnoki and D.L. Tárnoki were funded by the Bólyai scholarship of the Hungarian Academy of Sciences; and ÚNKP-20-5 and ÚNKP-21-5 New National Excellence Program of the Ministry for Innovation and Technology from the source of the National Research, Development, and Innovation Fund; and by the Hungarian National Laboratory (under the National Tumourbiology Laboratory project, NLP-17). M. Dąbrowska has nothing to disclose. M. Knetki-Wróblewska's conflicts of interest include being an invited speaker of MSD, BMS, Roche, AstraZeneca, Sanofi, Takeda, Pfizer, and receiving travel grants from MSD, Takeda, AstraZeneca and Pfizer. A. Frille reports a postdoctoral fellowship "MetaRot program" (clinician scientist program) from the Federal Ministry of Education and Research (BMBF), Germany (FKZ 01EO1501, IFB Adiposity Diseases), a research grant from the Mitteldeutsche Gesellschaft für Pneumologie (MDGP) e.V. (2018-MDGP-PA-002), a junior research grant from the Medical Faculty, University of Leipzig (934100-012), Germany, a graduate fellowship from the Novartis-Stiftung für therapeutische Forschung and funding from the "PETictCAC" project (ERA-PerMed_324), which was funded with tax funds on the basis of the budget passed by the Saxon State Parliament (Germany) under the frame of ERA PerMed (Horizon 2020). H. Stubbs reports grants from Janssen-Cliag Ltd (funding support

for unrelated study (2021)); and support for attending meetings and/or travel from Janssen-Cliag Ltd (support for attending ERS 2022, ERS 2021 and ATS 2021) and AOP (support for attending ERS 2023 and PH Academy 2023). K.G. Blyth reports grants from Rocket Medical and RS Oncology (research funding to institution); and other financial or non-financial interests as co-investigator of PREDICT-Meso international accelerator. A.D. Juul reports grants from the Danish Cancer Society and from the Danish Research Center for Lung Cancer; and reports that Medtronic has lent equipment to the Simulation Center at Odense University Hospital for a research project where she is the primary investigator.

Support statement: Á.D. Tárnoki and D.L. Tárnoki were funded by the Bólyai scholarship of the Hungarian Academy of Sciences; and ÚNKP-20-5 and ÚNKP-21-5 New National Excellence Program of the Ministry for Innovation and Technology from the source of the National Research, Development, and Innovation Fund, and by the Hungarian National Laboratory (under the National Tumourbiology Laboratory project, NLP-17). A. Frille was supported by the postdoctoral fellowship "MetaRot program" from the Federal Ministry of Education and Research (BMBF), Germany (FKZ 01EO1501, IFB Adiposity Diseases), a research grant from the Mitteldeutsche Gesellschaft für Pneumologie (MDGP) e.V. (2018-MDGP-PA-002), a junior research grant from the Medical Faculty, University of Leipzig (934100-012), a graduate fellowship from the Novartis-Stiftung für therapeutische Forschung (2023), and the "PETictCAC" project (ERA-PerMed_324), which was funded with tax funds on the basis of the budget passed by the Saxon State Parliament (Germany) under the frame of ERA PerMed (Horizon 2020).

References

1 Sung H, Ferlay J, Siegel RL, *et al.* Global cancer statistics 2020: GLOBOCAN estimates of incidence and mortality worldwide for 36 cancers in 185 countries. *CA Cancer J Clin* 2021; 71: 209–249.
2 De Wever W, Coolen J, Verschakelen JA. Imaging techniques in lung cancer. *Breathe* 2011; 7: 338–346.
3 Wu YJ, Wu FZ, Yang SC, *et al.* Radiomics in early lung cancer diagnosis: from diagnosis to clinical decision support and education. *Diagnostics (Basel)* 2022; 12: 1064.
4 Schaefer-Prokop C, Prokop M. New imaging techniques in the treatment guidelines for lung cancer. *Eur Respir J* 2002; 19: Suppl. 35, 71s–83s.
5 Nitrosi A, Borasi G, Nicoli F, *et al.* A filmless radiology department in a full digital regional hospital: quantitative evaluation of the increased quality and efficiency. *J Digit Imaging* 2007; 20: 140–148.
6 Lee W, Lee S, Chong S, *et al.* Radiation dose reduction and improvement of image quality in digital chest radiography by new spatial noise reduction algorithm. *PLoS One* 2020; 15: e0228609.
7 Kelcz F, Zink FE, Peppler WW, *et al.* Conventional chest radiography *vs* dual-energy computed radiography in the detection and characterization of pulmonary nodules. *AJR Am J Roentgenol* 1994; 162: 271–278.
8 Toyoda Y, Nakayama T, Kusunoki Y, *et al.* Sensitivity and specificity of lung cancer screening using chest low-dose computed tomography. *Br J Cancer* 2008; 98: 1602–1607.
9 Bradley SH, Abraham S, Callister ME, *et al.* Sensitivity of chest X-ray for detecting lung cancer in people presenting with symptoms: a systematic review. *Br J Gen Pract* 2019; 69: e827–e835.
10 National Institute for Health and Care Excellence (NICE). Suspected cancer: recognition and referral. Date last updated: 2 October 2023. Date last accessed: 7 October 2023. www.nice.org.uk/guidance/ng12
11 Mazzone PJ, Obuchowski N, Phillips M, *et al.* Lung cancer screening with computer aided detection chest radiography: design and results of a randomized, controlled trial. *PLoS One* 2013; 8: e59650.
12 Nam JG, Hwang EJ, Kim J, *et al.* AI improves nodule detection on chest radiographs in a health screening population: a randomized controlled trial. *Radiology* 2023; 307: e221894.
13 Purandare NC, Rangarajan V. Imaging of lung cancer: implications on staging and management. *Indian J Radiol Imaging* 2015; 25: 109–120.
14 MacDonald SL, Hansell DM. Staging of non-small cell lung cancer: imaging of intrathoracic disease. *Eur J Radiol* 2003; 45: 18–30.
15 Del Ciello A, Franchi P, Contegiacomo A, *et al.* Missed lung cancer: when, where, and why? *Diagn Interv Radiol* 2017; 23: 118–126.
16 Quekel LG, Kessels AG, Goei R, *et al.* Miss rate of lung cancer on the chest radiograph in clinical practice. *Chest* 1999; 115: 720–724.
17 Pantos I, Thalassinou S, Argentos S, *et al.* Adult patient radiation doses from non-cardiac CT examinations: a review of published results. *Br J Radiol* 2011; 84: 293–303.
18 Fujii K, Aoyama T, Yamauchi-Kawaura C, *et al*. Radiation dose evaluation in 64-slice CT examinations with adult and paediatric anthropomorphic phantoms. *Br J Radiol* 2009; 82: 1010–1018.
19 Mori S, Endo M, Nishizawa K, *et al*. Comparison of patient doses in 256-slice CT and 16-slice CT scanners. *Br J Radiol* 2006; 79: 56–61.
20 Ewaidat HA, Zheng X, Khader Y, *et al.* Assessment of radiation dose and image quality of multidetector computed tomography. *Iran J Radiol* 2018; 15: e59554.
21 Vonder M, Dorrius MD, Vliegenthart R. Latest CT technologies in lung cancer screening: protocols and radiation dose reduction. *Transl Lung Cancer Res* 2021; 10: 1154–1164.

22 Fischbach F, Knollmann F, Griesshaber V, *et al.* Detection of pulmonary nodules by multislice computed tomography: improved detection rate with reduced slice thickness. *Eur Radiol* 2003; 13: 2378–2383.
23 Bankier AA, MacMahon H, Goo JM, *et al.* Recommendations for measuring pulmonary nodules at CT: a statement from the Fleischner Society. *Radiology* 2017; 285: 584–600.
24 Wang Y, de Bock GH, van Klaveren RJ, *et al.* Volumetric measurement of pulmonary nodules at low-dose chest CT: effect of reconstruction setting on measurement variability. *Eur Radiol* 2010; 20: 1180–1187.
25 Goo JM, Tongdee T, Tongdee R, *et al.* Volumetric measurement of synthetic lung nodules with multi-detector row CT: effect of various image reconstruction parameters and segmentation thresholds on measurement accuracy. *Radiology* 2005; 235: 850–856.
26 Petrou M, Quint LE, Nan B, *et al.* Pulmonary nodule volumetric measurement variability as a function of CT slice thickness and nodule morphology. *AJR Am J Roentgenol* 2007; 188: 306–312.
27 MacMahon H, Naidich DP, Goo JM, *et al.* Guidelines for management of incidental pulmonary nodules detected on CT images: from the Fleischner Society 2017. *Radiology* 2017; 284: 228–243.
28 Cruickshank A, Stieler G, Ameer F. Evaluation of the solitary pulmonary nodule. *Intern Med J* 2019; 49: 306–315.
29 Chooi WK, Matthews S, Bull MJ, *et al.* Multislice computed tomography in staging lung cancer: the role of multiplanar image reconstruction. *J Comput Assist Tomogr* 2005; 29: 357–360.
30 Jankowski A, Martinelli T, Timsit JF, *et al.* Pulmonary nodule detection on MDCT images: evaluation of diagnostic performance using thin axial images, maximum intensity projections, and computer-assisted detection. *Eur Radiol* 2007; 17: 3148–3156.
31 De Wever W, Bogaert J, Verschakelen JA. Virtual bronchoscopy: accuracy and usefulness – an overview. *Semin Ultrasound CT MR* 2005; 26: 364–373.
32 Vervoorn MT, Wulfse M, Mohamed Hoesein FAA, *et al.* Application of three-dimensional computed tomography imaging and reconstructive techniques in lung surgery: a mini-review. *Front Surg* 2022; 9: 1079857.
33 Lederlin M, Revel MP, Khalil A, *et al.* Management strategy of pulmonary nodule in 2013. *Diagn Interv Imaging* 2013; 94: 1081–1094.
34 Lee D, Rho JY, Kang S, *et al.* CT findings of small cell lung carcinoma: can recognizable features be found? *Medicine (Baltimore)* 2016; 95: e5426.
35 Meisinger QC, Klein JS, Butnor KJ, *et al.* CT features of peripheral pulmonary carcinoid tumours. *AJR Am J Roentgenol* 2011; 197: 1073–1080.
36 Choi Y, Gil BM, Chung MH, *et al.* Comparing attenuations of malignant and benign solitary pulmonary nodule using semi-automated region of interest selection on contrast-enhanced CT. *J Thorac Dis* 2019; 11: 2392–2401.
37 Yuan R, Vos PM, Cooperberg PL. Computer-aided detection in screening CT for pulmonary nodules. *AJR Am J Roentgenol* 2006; 186: 1280–1287.
38 Hung SC, Wang YT, Tseng MH. An interpretable three-dimensional artificial intelligence model for computer-aided diagnosis of lung nodules in computed tomography images. *Cancers (Basel)* 2023; 15: 4655.
39 Goldstraw P, Chansky K, Crowley J, *et al.* The IASLC Lung Cancer Staging Project: proposals for revision of the TNM stage groupings in the forthcoming (eighth) edition of the TNM classification for lung cancer. *J Thorac Oncol* 2016; 11: 39–51.
40 Van Schil PE, Rami-Porta R, Asamura H. The 8th TNM edition for lung cancer: a critical analysis. *Ann Transl Med* 2018; 6: 87.
41 Matilla JM, Zabaleta M, Martínez-Téllez E, *et al.* New TNM staging in lung cancer (8th edition) and future perspectives. *J Clin Transl Res* 2020; 6: 145–154.
42 Glazer GM, Gross BH, Quint LE, *et al.* Normal mediastinal lymph nodes: number and size according to American Thoracic Society mapping. *AJR Am J Roentgenol* 1985; 144: 261–265.
43 Westeel V, Foucher P, Scherpereel A, *et al.* Chest CT scan plus X-ray *versus* chest X-ray for the follow-up of completely resected non-small-cell lung cancer (IFCT-0302): a multicentre, open-label, randomised, phase 3 trial. *Lancet Oncol* 2022; 23: 1180–1188.
44 Lell M, Kachelrieß M. Computed tomography 2.0: new detector technology, AI, and other developments. *Invest Radiol* 2023; 58: 587–601.
45 Scharm SC, Schaefer-Prokop C, Winther HB, *et al.* Regional pulmonary morphology and function: photon-counting CT assessment. *Radiology* 2023; 308: e230318.
46 Tortora M, Gemini L, D'Iglio I, *et al.* Spectral photon-counting computed tomography: a review on technical principles and clinical applications. *J Imaging* 2022; 8: 112.
47 Douek PC, Boccalini S, Oei EHG, *et al.* Clinical applications of photon-counting CT: a review of pioneer studies and a glimpse into the future. *Radiology* 2023; 309: e222432.
48 Kauczor HU, Ley-Zaporozhan J, Ley S. Imaging of pulmonary pathologies: focus on magnetic resonance imaging. *Proc Am Thorac Soc* 2009; 6: 458–463.

49 Bak SH, Kim C, Kim CH, *et al.* Magnetic resonance imaging for lung cancer: a state-of-the-art review. *Precis Future Med* 2022; 6: 49–77.
50 Ohno Y, Ozawa Y, Nagata H, *et al.* Lung magnetic resonance imaging: technical advancements and clinical applications. *Invest Radiol* 2024; 59: 38–52.
51 Campbell-Washburn AE, Ramasawmy R, Restivo MC, *et al.* Opportunities in interventional and diagnostic imaging by using high-performance low-field-strength MRI. *Radiology* 2019; 293: 384–393.
52 Schmidt GP, Reiser MF, Baur-Melnyk A. Whole-body MRI for the staging and follow-up of patients with metastasis. *Eur J Radiol* 2009; 70: 393–400.
53 Matoba M, Tonami H, Kondou T, *et al.* Lung carcinoma: diffusion-weighted MR imaging – preliminary evaluation with apparent diffusion coefficient. *Radiology* 2007; 243: 570–577.
54 Koh DM, Collins DJ. Diffusion-weighted MRI in the body: applications and challenges in oncology. *AJR Am J Roentgenol* 2007; 188: 1622–1635.
55 Ohno Y, Hatabu H, Takenaka D, *et al.* Solitary pulmonary nodules: potential role of dynamic MR imaging in management initial experience. *Radiology* 2002; 224: 503–511.
56 Sommer G, Tremper J, Koenigkam-Santos M, *et al.* Lung nodule detection in a high-risk population: comparison of magnetic resonance imaging and low-dose computed tomography. *Eur J Radiol* 2014; 83: 600–605.
57 Tanaka Y, Ohno Y, Hanamatsu S, *et al.* State-of-the-art MR imaging for thoracic diseases. *Magn Reson Med Sci* 2022; 21: 212–234.
58 Ciliberto M, Kishida Y, Seki S, *et al.* Update of MR imaging for evaluation of lung cancer. *Radiol Clin North Am* 2018; 56: 437–469.
59 Daly ME, Singh N, Ismaila N, *et al.* Management of stage III non-small-cell lung cancer: ASCO guideline. *J Clin Oncol* 2022; 40: 1356–1384.
60 Ohno Y, Koyama H, Nogami M, *et al.* Postoperative lung function in lung cancer patients: comparative analysis of predictive capability of MRI, CT, and SPECT. *AJR Am J Roentgenol* 2007; 189: 400–408.
61 Jagoda P, Fleckenstein J, Sonnhoff M, *et al.* Diffusion-weighted MRI improves response assessment after definitive radiotherapy in patients with NSCLC. *Cancer Imaging* 2021; 21: 15.
62 Novello S, Barlesi F, Califano R, *et al.* Metastatic non-small-cell lung cancer: ESMO Clinical Practice Guidelines for diagnosis, treatment and follow-up. *Ann Oncol* 2016; 27: Suppl. 5, v1–v27.
63 Remon J, Soria JC, Peters S, *et al.* Early and locally advanced non-small-cell lung cancer: an update of the ESMO Clinical Practice Guidelines focusing on diagnosis, staging, systemic and local therapy. *Ann Oncol* 2021; 32: 1637–1642.
64 National Comprehensive Cancer Network. NCCN Clinical Practice Guidelines in Oncology for Non-Small Cell Lung Cancer. Version: 3.2023. Date last accessed: 7 October 2023. www.nccn.org/guidelines/guidelines-detail?category=1&id=1450
65 Vander Heiden MG, Cantley LC, Thompson CB. Understanding the Warburg effect: the metabolic requirements of cell proliferation. *Science* 2009; 324: 1029–1033.
66 Lowe VJ, Hoffman JM, DeLong DM, *et al.* Semiquantitative and visual analysis of FDG-PET images in pulmonary abnormalities. *J Nucl Med* 1994; 35: 1771–1776.
67 Thie JA. Understanding the standardized uptake value, its methods, and implications for usage. *J Nucl Med* 2004; 45: 1431–1434.
68 Khalaf M, Abdel-Nabi H, Baker J, *et al.* Relation between nodule size and ^{18}F-FDG-PET SUV for malignant and benign pulmonary nodules. *J Hematol Oncol* 2008; 1: 13.
69 Boellaard R, Delgado-Bolton R, Oyen WJG, *et al.* FDG PET/CT: EANM procedure guidelines for tumour imaging: version 2.0. *Eur J Nucl Med Mol Imaging* 2015; 42: 328–354.
70 American College of Radiology. ACR–ACNM–SNMMI–SPR practice parameter for performing FDG-PET/CT in oncology. Date last updated: 2021. Date last accessed: 26 February 2024. https://www.acr.org/-/media/ACR/Files/Practice-Parameters/FDG-PET-CT.pdf
71 Chang JM, Lee HJ, Goo JM, *et al.* False positive and false negative FDG-PET scans in various thoracic diseases. *Korean J Radiol* 2006; 7: 57–69.
72 Gandy N, Arshad MA, Wallitt KL, *et al.* Immunotherapy-related adverse effects on ^{18}F-FDG PET/CT imaging. *Br J Radiol* 2020; 93: 20190832.
73 Sarikaya I, Albatineh AN, Sarikaya A. Revisiting weight-normalized SUV and lean-body-mass-normalized SUV in PET studies. *J Nucl Med Technol* 2020; 48: 163–167.
74 Eisenhauer EA, Therasse P, Bogaerts J, *et al.* New response evaluation criteria in solid tumours: revised RECIST guideline (version 1.1). *Eur J Cancer* 2009; 45: 228–247.
75 Seymour L, Bogaerts J, Perrone A, *et al.* iRECIST: guidelines for response criteria for use in trials testing immunotherapeutics. *Lancet Oncol* 2017; 18: e143–e152.
76 Hardavella G, Frille A, Theochari C, *et al.* Multidisciplinary care models for patients with lung cancer. *Breathe* 2020; 16: 200076.

77 Hope TA, Bergsland EK, Bozkurt MF, *et al.* Appropriate use criteria for somatostatin receptor PET imaging in neuroendocrine tumors. *J Nucl Med* 2018; 59: 66–74.

78 Lemjabbar-Alaoui H, Hassan OU, Yang YW, *et al.* Lung cancer: biology and treatment options. *Biochim Biophys Acta* 2015; 1856: 189–210.

79 Thureau S, Chaumet-Riffaud P, Modzelewski R, *et al.* Interobserver agreement of qualitative analysis and tumor delineation of ^{18}F-fluoromisonidazole and 3′-deoxy-3′-^{18}F-fluorothymidine PET images in lung cancer. *J Nucl Med* 2013; 54: 1543–1550.

80 Thureau S, Dubray B, Modzelewski R, *et al.* FDG and FMISO PET-guided dose escalation with intensity-modulated radiotherapy in lung cancer. *Radiat Oncol* 2018; 13: 208.

81 Even AJG, van der Stoep J, Zegers CML, *et al.* PET-based dose painting in non-small cell lung cancer: comparing uniform dose escalation with boosting hypoxic and metabolically active sub-volumes. *Radiother Oncol* 2015; 116: 281–286.

82 Watanabe S, Inoue T, Okamoto S, *et al.* Combination of FDG-PET and FMISO-PET as a treatment strategy for patients undergoing early-stage NSCLC stereotactic radiotherapy. *EJNMMI Res* 2019; 9: 104.

83 Salem A, Asselin MC, Reymen B, *et al.* Targeting hypoxia to improve non-small cell lung cancer outcome. *J Natl Cancer Inst* 2018; 110: 14–30.

84 Zegers CML, van Elmpt W, Wierts R, *et al.* Hypoxia imaging with [^{18}F]HX4 PET in NSCLC patients: defining optimal imaging parameters. *Radiother Oncol* 2013; 109: 58–64.

85 Bourigault P, Skwarski M, Macpherson RE, *et al.* Timing of hypoxia PET/CT imaging after ^{18}F-fluoromisonidazole injection in non-small cell lung cancer patients. *Sci Rep* 2022; 12: 21746.

86 Vera P, Thureau S, Chaumet-Riffaud P, *et al.* Phase II study of a radiotherapy total dose increase in hypoxic lesions identified by ^{18}F-misonidazole PET/CT in patients with non-small cell lung carcinoma (RTEP5 Study). *J Nucl Med* 2017; 58: 1045–1053.

87 Vera P, Mihailescu SD, Lequesne J, *et al.* Radiotherapy boost in patients with hypoxic lesions identified by ^{18}F-FMISO PET/CT in non-small-cell lung carcinoma: can we expect a better survival outcome without toxicity? (RTEP5 long-term follow-up). *Eur J Nucl Med Mol Imaging* 2019; 46: 1448–1456.

88 Watts A, Singh B, Singh H, *et al.* [^{68}Ga]Ga-Pentixafor PET/CT imaging for *in vivo* CXCR4 receptor mapping in different lung cancer histologic sub-types: correlation with quantitative receptors' density by immunochemistry techniques. *Eur J Nucl Med Mol Imaging* 2023; 50: 1216–1227.

89 National Lung Screening Trial Research Team, Aberle DR, Adams AM, *et al.* Reduced lung-cancer mortality with low-dose computed tomographic screening. *N Engl J Med* 2011; 365: 395–409.

90 US Preventive Services Task Force. Lung Cancer: Screening. Date last updated: 9 March 2021. Date last accessed: 7 October 2023. www.uspreventiveservicestaskforce.org/uspstf/recommendation/lung-cancer-screening

91 Kerpel-Fronius A, Monostori Z, Kovacs G, *et al.* Nationwide lung cancer screening with low-dose computed tomography: implementation and first results of the HUNCHEST screening program. *Eur Radiol* 2022; 32: 4457–4467.

92 American College of Radiology. Lung CT Screening Reporting and Data System (Lung-RADS). Date last accessed: 7 October 2023. www.acr.org/Clinical-Resources/Reporting-and-Data-Systems/Lung-Rads

93 Liang H, Hu M, Ma Y, *et al.* Performance of deep-learning solutions on lung nodule malignancy classification: a systematic review. *Life (Basel)* 2023; 13: 1911.

94 Hendrick RE, Smith RA. Benefit-to-radiation-risk of low-dose computed tomography lung cancer screening. *Cancer* 2023; 130: 216–223.

95 Pozzessere C, von Garnier C, Beigelman-Aubry C. Radiation exposure to low-dose computed tomography for lung cancer screening: should we be concerned? *Tomography* 2023; 9: 166–177.

96 Expert Panel on Thoracic Imaging, Martin MD, Henry TS, *et al.* ACR Appropriateness Criteria incidentally detected indeterminate pulmonary nodule. *J Am Coll Radiol* 2023; 20: Suppl. 11, S455–S470.

97 Macri F, Greffier J, Pereira FR, *et al.* Ultra-low-dose chest CT with iterative reconstruction does not alter anatomical image quality. *Diagn Interv Imaging* 2016; 97: 1131–1140.

98 Milanese G, Ledda RE, Sabia F, *et al.* Ultra-low dose computed tomography protocols using spectral shaping for lung cancer screening: comparison with low-dose for volumetric LungRADS classification. *Eur J Radiol* 2023; 161: 110760.

99 Gobi K, Arunachalam VK, Varatharajaperumal RK, *et al.* The role of ultra-low-dose computed tomography in the detection of pulmonary pathologies: a prospective observational study. *Pol J Radiol* 2022; 87: e597–e605.

100 Hansell DM, Bankier AA, MacMahon H, *et al.* Fleischner Society: glossary of terms for thoracic imaging. *Radiology* 2008; 246: 697–722.

101 Gould MK, Donington J, Lynch WR, *et al.* Evaluation of individuals with pulmonary nodules: when is it lung cancer? Diagnosis and management of lung cancer, 3rd ed: American College of Chest Physicians evidence-based clinical practice guidelines. *Chest* 2013; 143: e93S–e120S.

102 Baldwin DR, Callister MEJ, Guideline Development Group. The British Thoracic Society guidelines on the investigation and management of pulmonary nodules. *Thorax* 2015; 70: 794–798.

103 Naidich DP, Bankier AA, MacMahon H, *et al.* Recommendations for the management of subsolid pulmonary nodules detected at CT: a statement from the Fleischner Society. *Radiology* 2013; 266: 304–317.

104 Ost DE, Gould MK. Decision making in patients with pulmonary nodules. *Am J Respir Crit Care Med* 2012; 185: 363–372.

105 Swensen SJ, Silverstein MD, Ilstrup DM, *et al.* The probability of malignancy in solitary pulmonary nodules. Application to small radiologically indeterminate nodules. *Arch Intern Med* 1997; 157: 849–855.

106 van Riel SJ, Ciompi F, Jacobs C, *et al.* Malignancy risk estimation of screen-detected nodules at baseline CT: comparison of the PanCan model, Lung-RADS and NCCN guidelines. *Eur Radiol* 2017; 27: 4019–4029.

107 González Maldonado S, Delorme S, Hüsing A, *et al.* Evaluation of prediction models for identifying malignancy in pulmonary nodules detected *via* low-dose computed tomography. *JAMA Netw Open* 2020; 3: e1921221.

108 Cronin P, Dwamena BA, Kelly AM, *et al.* Solitary pulmonary nodules: meta-analytic comparison of cross-sectional imaging modalities for diagnosis of malignancy. *Radiology* 2008; 246: 772–782.

109 Gould MK, Maclean CC, Kuschner WG, *et al.* Accuracy of positron emission tomography for diagnosis of pulmonary nodules and mass lesions: a meta-analysis. *JAMA* 2001; 285: 914–924.

110 Cieszanowski A, Lisowska A, Dabrowska M, *et al.* MR imaging of pulmonary nodules: detection rate and accuracy of size estimation in comparison to computed tomography. *PLoS One* 2016; 11: e0156272.

111 Ohno Y, Koyama H, Yoshikawa T, *et al.* Standard-, reduced-, and no-dose thin-section radiologic examinations: comparison of capability for nodule detection and nodule type assessment in patients suspected of having pulmonary nodules. *Radiology* 2017; 284: 562–573.

112 Sacchi de Camargo Correia G, Pai T, Li S, *et al.* Immune-related adverse events in patients with lung cancer. *Curr Oncol Rep* 2023; 25: 1259–1275.

113 Suresh K, Voong KR, Shankar B, *et al.* Pneumonitis in non-small cell lung cancer patients receiving immune checkpoint immunotherapy: incidence and risk factors. *J Thorac Oncol* 2018; 13: 1930–1939.

114 Chen X, Sheikh K, Nakajima E, *et al.* Radiation *versus* immune checkpoint inhibitor associated pneumonitis: distinct radiologic morphologies. *Oncologist* 2021; 26: e1822–e1832.

115 Naidoo J, Wang X, Woo KM, *et al.* Pneumonitis in patients treated with anti-programmed death-1/programmed death ligand 1 therapy. *J Clin Oncol* 2017; 35: 709–717.

116 Machtay M, Teba CV. 47 – Pulmonary complications of anticancer treatment. *In*: Niederhuber JE, Armitage JO, Doroshow JH, *et al.*, eds. Abeloff's Clinical Oncology. 6th Edn. Philadelphia, Elsevier, 2020; pp. 715–724.e2.

117 Zhang J, Qiu T, Zhou Y, *et al.* Tyrosine kinase inhibitors-associated interstitial lung disease used in non-small cell lung cancer: a pharmacovigilance analysis based on the FDA adverse event reporting system database. *Expert Opin Drug Saf* 2023; 22: 849–856.

118 Chen B, Zhang R, Gan Y, *et al.* Development and clinical application of radiomics in lung cancer. *Radiat Oncol* 2017; 12: 154.

119 Walls GM, Osman SOS, Brown KH, *et al.* Radiomics for predicting lung cancer outcomes following radiotherapy: a systematic review. *Clin Oncol* 2022; 34: e107–e122.

120 Hu Q, Li K, Yang C, *et al.* The role of artificial intelligence based on PET/CT radiomics in NSCLC: disease management, opportunities, and challenges. *Front Oncol* 2023; 13: 1133164.

121 Chetan MR, Gleeson FV. Radiomics in predicting treatment response in non-small-cell lung cancer: current status, challenges and future perspectives. *Eur Radiol* 2021; 31: 1049–1058.

122 Chen Q, Zhang L, Mo X, *et al.* Current status and quality of radiomic studies for predicting immunotherapy response and outcome in patients with non-small cell lung cancer: a systematic review and meta-analysis. *Eur J Nucl Med Mol Imaging* 2021; 49: 345–360.

123 Wang S, Yu H, Gan Y, *et al.* Mining whole-lung information by artificial intelligence for predicting EGFR genotype and targeted therapy response in lung cancer: a multicohort study. *Lancet Digit Health* 2022; 4: e309–e319.

124 Zhang T, Xu Z, Liu G, *et al.* Simultaneous identification of *EGFR*, *KRAS*, *ERBB2*, and *TP53* mutations in patients with non-small cell lung cancer by machine learning-derived three-dimensional radiomics. *Cancers (Basel)* 2021; 13: 1814.

125 Shao J, Ma J, Zhang S, *et al.* Radiogenomic system for non-invasive identification of multiple actionable mutations and PD-L1 expression in non-small cell lung cancer based on CT images. *Cancers (Basel)* 2022; 14: 4823.

126 Chandrasekhar AJ, Reynes CJ, Churchill RJ. Ultrasonically guided percutaneous biopsy of peripheral pulmonary masses. *Chest* 1976; 70: 627–630.

127 Laursen CB, Naur TM, Bodtger U, *et al.* Ultrasound-guided lung biopsy in the hands of respiratory physicians: diagnostic yield and complications in 215 consecutive patients in 3 centers. *J Bronchology Interv Pulmonol* 2016; 23: 220–228.

128 Jacobsen N, Pietersen PI, Nolsoe C, *et al.* Clinical applications of contrast-enhanced thoracic ultrasound (CETUS) compared to standard reference tests: a systematic review. *Ultraschall Med* 2022; 43: 72–81.

129 Vilmann P, Clementsen PF, Colella S, *et al.* Combined endobronchial and oesophageal endosonography for the diagnosis and staging of lung cancer. European Society of Gastrointestinal Endoscopy (ESGE) Guideline, in cooperation with the European Respiratory Society (ERS) and the European Society of Thoracic Surgeons (ESTS). *Eur Respir J* 2015; 46: 40–60.

130 Wahidi MM, Herth F, Yasufuku K, *et al.* Technical aspects of endobronchial ultrasound-guided transbronchial needle aspiration: CHEST guideline and expert panel report. *Chest* 2016; 149: 816–835.

131 Christiansen IS, Ahmad K, Bodtger U, *et al.* EUS-B for suspected left adrenal metastasis in lung cancer. *J Thorac Dis* 2020; 12: 258–263.

132 Christiansen IS, Bodtger U, Naur TMH, *et al.* EUS-B-FNA for diagnosing liver and celiac metastases in lung cancer patients. *Respiration* 2019; 98: 428–433.

133 Issa MA, Sidhu JS, Tehrani SG, *et al.* Endoscopic ultrasound-guided pancreas biopsy in the hands of a chest physician. *Respir Med Case Rep* 2023; 43: 101833.

134 Steinfort DP, Farmer MW, Irving LB, *et al.* Pulmonologist-performed per-esophageal needle aspiration of parenchymal lung lesions using an EBUS bronchoscope: diagnostic utility and safety. *J Bronchology Interv Pulmonol* 2017; 24: 117–124.

135 Planchard D, Popat S, Kerr K, *et al.* Metastatic non-small cell lung cancer: ESMO Clinical Practice Guidelines for diagnosis, treatment and follow-up. *Ann Oncol* 2018; 29: Suppl. 4, iv192–iv237.

136 Deng CJ, Dai FQ, Qian K, *et al.* Clinical updates of approaches for biopsy of pulmonary lesions based on systematic review. *BMC Pulm Med* 2018; 18: 146.

137 Schreiber G, McCrory DC. Performance characteristics of different modalities for diagnosis of suspected lung cancer: summary of published evidence. *Chest* 2003; 123: Suppl. 1, 115S–128S.

138 Huang ZG, Sun HL, Wang CL, *et al.* CT-guided transthoracic needle biopsy of pulmonary lesions: comparison between the cutting needle and aspiration needle. *Br J Radiol* 2021; 94: 20190930.

139 Takeshita J, Masago K, Kato R, *et al.* CT-guided fine-needle aspiration and core needle biopsies of pulmonary lesions: a single-center experience with 750 biopsies in Japan. *AJR Am J Roentgenol* 2015; 204: 29–34.

140 Wu CC, Maher MM, Shepard J-AO. Complications of CT-guided percutaneous needle biopsy of the chest: prevention and management. *AJR Am J Roentgenol* 2011; 196: W678–W682.

141 Covey AM, Gandhi R, Brody LA, *et al.* Factors associated with pneumothorax and pneumothorax requiring treatment after percutaneous lung biopsy in 443 consecutive patients. *J Vasc Interv Radiol* 2004; 15: 479–483.

142 Mills M, Choi J, El-Haddad G, *et al.* Retrospective analysis of technical success rate and procedure-related complications of 867 percutaneous CT-guided needle biopsies of lung lesions. *Clin Radiol* 2017; 72: 1038–1046.

143 Ozturk K, Soylu E, Gokalp G, *et al.* Risk factors of pneumothorax and chest tube placement after computed tomography-guided core needle biopsy of lung lesions: a single-centre experience with 822 biopsies. *Pol J Radiol* 2018; 83: e407–e414.

144 García-Río F, Pino JM, Casadevall J, *et al.* Use of spirometry to predict risk of pneumothorax in CT-guided needle biopsy of the lung. *J Comput Assist Tomogr* 1996; 20: 20–23.

145 Ruud EA, Heck S, Stavem K, *et al.* Low diffusion capacity of the lung predicts pneumothorax and chest drainage after CT-guided lung biopsy. *BMC Res Notes* 2022; 15: 353.

146 Ost DE, Ernst A, Lei X, *et al.* Diagnostic yield and complications of bronchoscopy for peripheral lung lesions. Results of the AQuIRE Registry. *Am J Respir Crit Care Med* 2016; 193: 68–77.

147 Thiboutot J, Pastis NJ, Akulian J, *et al.* A multicenter, single-arm, prospective trial assessing the diagnostic yield of electromagnetic bronchoscopic and transthoracic navigation for peripheral pulmonary nodules. *Am J Respir Crit Care Med* 2023; 208: 837–845.

148 Pertzov B, Gershman E, Izhakian S, *et al.* The LungVision navigational platform for peripheral lung nodule biopsy and the added value of cryobiopsy. *Thorac Cancer* 2021; 12: 2007–2012.

149 Casal RF, Sarkiss M, Jones AK, *et al.* Cone beam computed tomography-guided thin/ultrathin bronchoscopy for diagnosis of peripheral lung nodules: a prospective pilot study. *J Thorac Dis* 2018; 10: 6950–6959.

150 Salahuddin M, Bashour SI, Khan A, *et al.* Mobile cone-beam CT-assisted bronchoscopy for peripheral lung lesions. *Diagnostics (Basel)* 2023; 13: 827.

151 Chen AC, Pastis NJ Jr, Mahajan AK, *et al.* Robotic bronchoscopy for peripheral pulmonary lesions: a multicenter pilot and feasibility study (BENEFIT). *Chest* 2021; 159: 845–852.

152 Celikoglu F, Celikoglu SI, Goldberg EP. Intratumoural chemotherapy of lung cancer for diagnosis and treatment of draining lymph node metastasis. *J Pharm Pharmacol* 2010; 62: 287–295.

153 Aryal S, Park S, Park H, *et al.* Clinical trials for oral, inhaled and intravenous drug delivery system for lung cancer and emerging nanomedicine-based approaches. *Int J Nanomedicine* 2023; 18: 7865–7888.

Suggested answers

1. Chest radiography has a limited sensitivity: in the "blind zones" on postero-anterior chest radiographs; for prediction of T3 and T4 disease; for prediction of the invasion of the chest wall, diaphragm and mediastinum, and nodal involvement; and for small tumour size (diameter ⩽10 mm).
2. The advantages of PCCT are: absence of electronic noise, improved radiation dose efficiency, increased iodine signal, lower doses of iodinated contrast material administration, better spatial resolution, spectral imaging, and the possibility of acquiring quantitative functional data such as lung perfusion.
3. The current roles of lung MRI in lung cancer imaging include: determination of tumour invasion in the chest wall and the mediastinal structures; differentiation between solid and vascular hilar masses; assessment of tumour cellularity; possible characterisation of different subtypes; N- and M-stage evaluation, *e.g.* screening for brain, vertebral/spine metastasis; assessment of distant metastatic disease; assessment of diaphragmatic abnormalities; and differentiation of lung cancer from progressive massive fibrosis, tuberculomas and obstructive pneumonia, and from surrounding post-obstructive atelectasis.
4. Advantages: good sensitivity and specificity in successfully diagnosing early-stage lung cancers; low radiation dose. Disadvantages: indication of unnecessary invasive procedures or complications due to the high malignancy-related false-positive rate.
5. The role of radiomics/radiogenomics is to aggregate radiology and genomics data with the aim of predicting the macroscopic and molecular properties of tissues. In the near future, it is likely to have a major impact on diagnostic and treatment pathways for lung cancer.
6. Ultrasound- and CT-guided biopsy, ablation, intratumoural injection of cytotoxic drugs into endobronchial tumours through a bronchoscope, targeted therapy and immunotherapy.